Geoderma 438 (2023) 116635

Contents lists available at ScienceDirect

Geoderma

journal homepage: www.elsevier.com/locate/geoderma

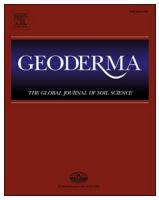

Effects of different land-use types on the activity and community of autotrophic microbes in karst soil

Xing Liu [a,b,c], Qiusheng Wu [a], Heng Wang [a,c], Yuan Zhao [a,c], Zaihua Liu [a,d], Quan Yuan [a,d,*]

[a] State Key Laboratory of Environmental Geochemistry, Institute of Geochemistry, Chinese Academy of Sciences, Guiyang 550081, China
[b] School of Geography and Resources, Guizhou Education University, Guiyang 550018, China
[c] University of Chinese Academy of Sciences, Beijing 100049, China
[d] Puding Karst Ecosystem Research Station, Chinese Ecosystem Research Network, Chinese Academy of Sciences, Puding, Guizhou 562100, China

ARTICLE INFO

Handling Editor: M. Tighe.

Keywords:
Autotrophic carbon fixation
Autotrophic community
$^{13}CO_2$ labelling
Soil organic carbon
Karst soil

ABSTRACT

CO_2 fixation by soil autotrophic microbes could make considerable contribution to soil organic matter (SOM). However, the effects of different land-use types on the activity and community of soil autotrophic microbes are still unclear. In this study, the autotrophic carbon fixation (ACF) rates of karst soils with four land-use types were assessed by $^{13}CO_2$ labelling. After 21 days incubation under alternate 12 h light with darkness, the ACF rate was 0.18 mg C·kg^{-1}·day^{-1} in bare land soil, approximately 0.39 mg C·kg^{-1}·day^{-1} in crop land and shrub land soils, while sharply increased to 1.54 mg C·kg^{-1}·day^{-1} in grass land soil. The ^{13}C nuclear magnetic resonance analysis of SOM showed that the fixed $^{13}CO_2$ was mainly incorporated into carbonyl carbon in grass land soil, but largely incorporated into recalcitrant aromatic carbon in other land-use types, especially in bare land. Longer incubation time (21 days versus 7 days) greatly elevated ACF rate only in grass land soil (by about 4 times) under continuous light conditions, suggesting that longer incubation in light conditions largely stimulated microbial phototrophic CO_2 fixation in grass land soil. Metagenomic analysis showed that the soil autotrophic microbial communities were prominently different among the four land-use types, and the autotrophic populations using bicarbonate as inorganic carbon species were most important for explaining the variations of autotrophic communities among the land-use types. Additionally, total nitrogen and soil organic carbon contents could be the key controlling factors of both ACF rates and structure of autotrophic microbial communities. Eventually, the change of soil properties caused by land-use type substantially affected the activity and community of soil autotrophic microbes, as well as the fate and stability of the assimilated CO_2.

1. Introduction

Increasing evidences have shown the importance of microbial autotrophic carbon fixation (ACF) capacity in different soils (Ge et al., 2013; Nowak et al., 2015; Liu et al., 2018). A recent study found that ACF in situ accounted for 18.2% of plant gross primary productivity in dryland ecosystem (Chen et al., 2021). And global soil autotrophic microbes are roughly estimated to fix up to 4.9 Pg C per year (Yuan et al., 2012). In addition, both chemolithotrophic and phototrophic carbon fixation by microbes were considered to play an indispensable role in soil carbon cycling (Miltner et al., 2005; Ge et al., 2013).

Microbial autotrophic metabolism can convert CO_2 into soil organic matter (SOM) in the continuous iterative processes of cell generation, population growth and death (Liang et al., 2017). In wetland soil, 27% of SOM in the 0–10 cm layer was considered derived from microbial assimilated CO_2 (Nowak et al., 2015). Moreover, ^{13}C nuclear magnetic resonance (^{13}C NMR) analysis of SOM indicated that autotrophic microbes assimilate CO_2 into alkyl and alkoxyl carbon of lipids, carbohydrates and proteins (Hart et al., 2013; Kelleher et al., 2017). Besides, the $^{14}CO_2$ isotope tracer experiment showed that more than 70% of ^{14}C-SOC (soil organic carbon) in paddy soils was concentrated in humin, a relatively stable humus fraction (Xiao et al., 2020).

Autotrophic microbes could assimilate CO_2 employing the following six pathways: the Calvin-Benson-Bassham (CBB) cycle, the reductive acetyl-CoA or Wood-Ljungdahl pathway (WL), the reductive tricarboxylic acid cycle (rTCA), the 3-hydroxypropionate/malyl-CoA cycle (3-HP), the 3-hydroxypropionate/4-hydroxybutyrate cycle (3-HP/4-HB), and the dicarboxylate/4-hydroxybutyrate cycle (DC/4-HB) (Berg et al.,

* Corresponding author at: State Key Laboratory of Environmental Geochemistry, Institute of Geochemistry, Chinese Academy of Sciences, Guiyang 550081, China.
E-mail address: yuanquan@mail.gyig.ac.cn (Q. Yuan).

https://doi.org/10.1016/j.geoderma.2023.116635
Received 23 August 2022; Received in revised form 16 June 2023; Accepted 3 August 2023
Available online 14 August 2023

2011; Hügler and Sievert, 2011). In addition, the pathway of chemolithoautotrophic phosphite oxidation was also detected in anaerobic wastewater treatment sludge, which may be the seventh natural CO_2 fixation pathway (Figueroa et al., 2018). Earlier studies normally targeted functional genes of individual carbon fixation pathway to investigate the phylogenetic diversity of autotrophic microbes (Wu et al., 2015; Zhao et al., 2020). Recently, metagenomics has been used to comprehensively analyze the autotrophic microbial communities and carbon fixation pathway in desert, forest and farmland soil (Bay et al., 2021; Chen et al., 2021).

It is widely reported that different fertilization management and cropping system could change soil properties, such as pH, microbial biomass carbon (MBC) and SOC (Wu et al., 2015; Burst et al., 2020), which were found to influence the activity and community of autotrophic carbon fixation (Long et al., 2015; Zhao et al., 2018). However, little is known about the effects of different land-use types on the carbon fixation capacity and community of autotrophic microbes. We hypothesized that land-use type would substantially affect the activity and community of soil autotrophic microbes, as well as fate of the fixed CO_2. To test this hypothesis, we targeted on soils of four simulated land-use types (grass land, shrub land, crop land and bare land) located in karst area of Southwest China, which is the largest karst area in the world and a typical ecologically fragile area with the strongest karst development (Li et al., 2021). We used $^{13}CO_2$ labelling approach in conditions with and without light together with CP-MAS ^{13}C NMR, to determine the ACF rates and its contribution to SOM components, and deep shotgun metagenomic sequencing was applied to determine the autotrophic community and carbon fixation pathways of these soils.

2. Materials and methods

2.1. The simulation test site and soil sampling

The simulation test site (26°14′ – 26°15′N, 105°42′ – 105°43′E) is located at the Puding Comprehensive Karst Research and Experimental Station, Guizhou Province, China. Guizhou Province belongs to humid subtropical monsoon climate with an annual average air temperature of about 15.1 °C and a mean annual average rainfall of 1315 mm, 80% of which occurs during the rainy season from May to October. The simulation test site consists of five adjoining concrete tanks (each 20 m long, 5 m wide and 3 m deep), so as to simulate five different land-use types (Fig. S1): Bare rock, bare land, crop land, grass land and shrub land soil (Zeng et al., 2017). The tanks are filled with dolomitic limestone rubble of 2.5 m depth topped with calcareous soil of 0.5 m, except that the tank for bare rock is only filled with rubble. The 2.5 m dolomitic limestone rubble and 0.5 m soil are identical in all tanks, so as to largely reduce the spatial heterogeneity of soil and rock within and among the different tanks. The weeds are regularly removed from bare land soil. The corn is planted in crop land every year since 2014, the growing season of corn is from May to August. The *Alfalfa* and *Rosa roxburghii* were planted in grass land and shrub land in January 2014, respectively. The four vegetation types are typical land-use types in karst ecosystem (Peng and Wang, 2012). Soil samples were collected in August 2018 from the four land-use types (bare land, crop land, grass land and shrub land), except the bare rock without soil. Topsoil (0–5 cm) was collected from 5 sampling points in each land-use type, then thoroughly mixed and sieved through a 2.0 mm sieve to prepare representative soil sample of each land-use type, which is important for the subsequent experiments and analyses related with soil incubation.

2.2. Soil properties analyses

Soil pH was determined by a pH meter (Shanghai dap PHS-3C, China) using soil to water ratio of 1:2.5. After extraction by 2 M KCl (soil/solution, 1:5), the contents of nitrate and sulfate were determined by ion chromatography (DIONEX ICS-90), and the content of ammonium was measured by Nessler's reagent colorimetry. Soil organic carbon (SOC) and total nitrogen (TN) contents were measured by Vario MACRO cube (Elementar, Germany) after added 0.5 M HCl to 1 g freeze-dried soil, adjusted to pH 2–3, and then washed to neutral. Dissolved organic carbon (DOC) was extracted by adding 20 ml 0.05 M K_2SO_4 to 5 g fresh soil (dry weight), shaking at 250 rpm for 30 min, and then filtering with Whatman GF/F filter papers. Finally, DOC was determined by an automated procedure using the vario TOC liquid mode (Elementar, Germany). Soil particle size was determined by a Laser scattering particle analyzer (Beckman Coulter, U.S.A).

The soil properties are given in Table 1: The SOC contents of the four land-use types ranged from 18.18 $g{\cdot}kg^{-1}$ to 34.09 $g{\cdot}kg^{-1}$, the DOC ranged from 74.63 $mg{\cdot}kg^{-1}$ to 202.95 $mg{\cdot}kg^{-1}$, and the TN ranged from 1.63 $g{\cdot}kg^{-1}$ to 3.14 $g{\cdot}kg^{-1}$. These parameters were lowest in bare land soil but highest in grass land soil (Table 1, $p < 0.05$), while the contents of clay were similar (about 80%) among the four land-use types.

2.3. Soil $^{13}CO_2$ labelling

Soils were adjusted to constant moisture (60% of field capacity) and preincubated in darkness at 25 °C for 2 days. For each soil sample, 10 g (dry weight) fresh soil was added into a 120 ml transparent serum bottle sealed with a rubber stopper and aluminum cap. To measure ACF rate and trace the fixed carbon, we added 5% (v/v) $^{13}CO_2$ (99 atom %, Cambridge Isotope Laboratories, USA) into the bottle as described previously (Long et al., 2015; Zhao et al., 2018), and we also prepared control sets with 5% (v/v) $^{12}CO_2$ or ambient air. Three treatments were prepared as described below. The first treatment was incubated in alternate 12 h light (15000 LX) with darkness; the second treatment was incubated in continuous darkness; and the third treatment was cultivated in continuous light conditions (15000 LX). The treatment with alternate light and darkness was adopted to simulate the carbon fixation in natural conditions, and the continuous darkness and light were prepared to investigate the differences in the carbon fixation between chemolithotrophic and phototrophic microbes. Three replicates were prepared for each treatment. All bottles were cultivated in artificial climate box (BIC-300, CHANGLIU, China) at 25 °C. The accumulation of CO_2 in the bottle with ambient air was monitored during the incubation, and the bottles were flushed with fresh air every 7 days to maintain

Table 1
Soil properties of the four land-use types.

	Bare land	Crop land	Shrub land	Grass land
pH	6.97±0.00 d	7.01 ±0.02c	7.13±0.03b	6.86±0.00 a
Ammonium ($mg{\cdot}kg^{-1}$)	3.92 ±0.01b	3.44 ±0.21b	3.94±0.34b	9.15±0.89 a
Nitrate ($mg{\cdot}kg^{-1}$)	27.84 ±0.21b	16.83 ±1.81c	8.63±1.50c	253.14 ±11.06 a
TN ($g{\cdot}kg^{-1}$)	1.63 ±0.54c	1.92 ±0.05b	1.72±0.08c	3.14±0.09 a
Sulfate ($mg{\cdot}kg^{-1}$)	5.89 ±2.50b	3.44 ±0.20c	3.23±0.31c	13.86±1.62 a
SOC ($g{\cdot}kg^{-1}$)	18.18 ±0.09c	21.38 ±0.61b	22.00±1.03b	34.09±1.59 a
C/N	11.14 ±0.92b	11.16 ±0.09b	12.77±0.23 a	10.86±0.63b
DOC ($mg{\cdot}kg^{-1}$)	74.63 ±0.55c	99.90 ±4.53b	110.38 ±11.40b	202.95±8.85 a
Clay (<2 μm, %)	78.47 ±2.27 a	80.53 ±2.24 a	78.51±0.64 a	81.39±0.25 a
Silt (2–50 μm, %)	21.52 ±2.27 a	19.46 ±2.24 a	21.48±0.64 a	18.60±0.25 a

Data represent the means ± SD (standard deviation, n = 3). TN, total nitrogen; SOC, soil organic carbon; C/N, the ratio of SOC and TN contents; DOC, soil dissolved organic carbon. The differences in each parameter among the four land-use types were tested by one-way ANOVA, and different letters indicate significant difference (Duncan; $p < 0.05$) between the data.

aerobic condition. Then the $^{13}CO_2$ or $^{12}CO_2$ was reinjected into the corresponding bottles as described above. The soil samples were destructively collected after 7 days and 21 days of incubation. Considering that longer incubation could be helpful for investigating the distribution of the fixed CO_2 in SOM, more parameters were analyzed for the soil samples incubated for 21 days, while the samples collected at day 7 only determined the δ^{13}C-SOC values which were used for calculating the ACF rates. When the bottles were opened for sampling, 5 g soil sample was stored at 4 °C for δ^{13}C-DOC measurement, and the rest of the sample was immediately freeze-dried for analyses associated with SOC.

2.4. Soil $^{13}CO_2$ fixation rate assessment

After acidification and lyophilization, δ^{13}C values of the SOC and DOC were determined using combustion-isotope ratio mass spectrometry system (EA-C-IRMS, Finnigan, Bremen, Germany). The $^{13}CO_2$ fixation capacity, i.e. the ACF rate (mg C·kg^{-1}·day^{-1}) was calculated according to the enrichment in ^{13}C atom% of SOC after $^{13}CO_2$ labelling (Long et al., 2015; Zhao et al., 2020). The rate of $^{13}CO_2$ incorporated into DOC was calculated with similar way.

2.5. The CP-MAS ^{13}C NMR analysis

4 g freeze-dried soil sample was placed into 50 ml polypropylene centrifuge tubes with 1.39 M HCl and 5 M HF, maintaining soil/solution ratio of 1:10, and then shaking for 48 h (Salati et al., 2008; Hart et al., 2013). After that, the sample was centrifuged at 6400 g for 20 min, and then the supernatant was discarded. The procedure was repeated four times to remove silicates and other magnetic minerals. The samples were neutralized by adding sterile ultrapure water until the pH value of the supernatant reached 6. Then, the soil sample was collected by centrifugation and lyophilization.

The soil CP-MAS ^{13}C NMR spectra were obtained on Bruker AVANCE III 400 spectrometer (Bruker BioSpin AG, Fällanden, Switzerland) equipped with a 4 mm standard bore CP-MAS probe head whose X channel was tuned to 100.62 MHz for ^{13}C, using a magnetic field of 9.39 T at 297 K. The dried and finely powdered samples were packed in the ZrO_2 rotor closed with Kel-F cap which were spun at 8 kHz rate. The experiments were conducted at a contact time of 2 ms. A total of 10,000 scans were recorded with 3 s recycle delay for each sample. All ^{13}C CP-MAS chemical shifts are referenced to the resonances of adamantane ($C_{10}H_{16}$) standard (δ_{CH2} = 38.4). All ^{13}C NMR spectra baselines were manually corrected and phased, subsequently we quantified the respective areas by integration.

To quantify different carbon components, we divided each spectrum into four chemical shift regions, which represent specific chemical carbon structures (Prietzel et al., 2018). (1) The chemical shift region 0–45 ppm represents alkyl carbon. (2) The region 45–110 ppm represents alkoxyl carbon. (3) The region 110–160 ppm represents aromatic carbon. (4) The region 160–220 ppm represents carbonyl carbon.

2.6. DNA extraction and metagenomic sequencing

Total soil DNA was extracted from approximately 500 mg uncultured soil samples using the E.Z.N.A.® Soil DNA Kit (OMEGA Bio-Tek, USA) according to the manufacturer's protocol. Three replicates were prepared for the soil of each land-use types. 500 ng qualified DNA per sample was fragmented by sonication to generate approximately 500 bp fragments, and sequencing libraries were prepared using the NEB Next® Ultra™ DNA Library Prep Kit for Illumina® (NEB, USA) following manufacturer's instructions. Sequencing was conducted by Illumina HiSeq X ten at Sangon Biotech Co., Ltd. (Shanghai, China). In addition, the *cbbL* gene, which is a marker gene of CBB cycle, was amplified with the primer pair of *cbbL*_K2f (5′-ACCAYCAAGCCSAAGCTSGG-3′) and *cbbL*_V2r (5′-GCCTTCSAGCTTGCCSACCRC-3′) (Zhao et al., 2020), and sequenced on an Illumina MiSeq platform at Shanghai Sangon Biotech Co., Ltd. (Shanghai, China).

2.7. Metagenomic data analysis

The clean reads were assembled using IDBA_UD software based on the *De Bruijn graph* (Peng et al., 2012). According to overlap between reads, we obtained contigs, and selected the best kmer assembly results. Contigs longer than 500 bp were used for further analysis. The open reading frames (ORFs) in the contigs were predicted using Prodigal and genes ≥100 bp were translated into protein sequences. Detailed information about metagenome datasets are shown in Table S1. The relative gene abundance was defined by SAMtools after comparing the clean reads of each sample with the non-redundant gene set through Bowtie2 (Langmead and Salzberg, 2012). For taxonomic analysis, the unique contigs were compared against the Nr (non-redundant protein sequences) datasets of the National Center for Biotechnology Information (NCBI) with microbial reference genomes using DIAMOND (Degnan and Ochman, 2012). The resulting alignment hits with e-values larger than 1×10^{-5} and scores <60 were filtered out. The lowest common ancestor (LCA) algorithm for MEGAN was used to identify every contig taxon (Huson et al., 2011). Predicted ORFs were clustered in CD-HIT with default parameters (Karlsson et al., 2013). GhostKOALA was used for amino acid alignment against the Kyoto Encyclopedia of Genes and Genomes (KEGG, https://www.genome.jp/kegg/) (Kanehisa and Goto, 2000). The putative autotrophic microbes were determined according to six carbon fixation pathways of M00165 (CBB cycle), M00173 (rTCA cycle), M00374 (DC/4-HB cycle), M00375 (3-HP/4-HB cycle), M00376 (3-HP cycle), and M00377 (WL pathway) in KEGG (Berg, 2011; Liu et al., 2018). Furthermore, the putative autotrophic microbes were screened from ORF annotation based on the modules M00528 (nitrification), M00804 (complete nitrification) and M00595 (thiosulfate oxidation by SOX complex). The relative abundances of taxonomic affiliations, which were selected from the corresponding KEGG Orthology (KO) of key enzyme of autotrophic carbon fixation pathway (Kanehisa et al., 2004; Ortiz et al., 2014; Ruiz-Fernandez et al., 2020), reflected the representative taxa of homologous pathway and its variation in four land-use types. In addition, all *cbbL* raw sequences were quality-filtered, chimera checked and the operational taxonomic units (OTUs) table was created using Usearch v9.2.64 (Edgar, 2010). The metagenomic data have been submitted to the NCBI with the BioProject ID: PRJNA666015.

2.8. Binning of metagenomic data

High-quality metagenomic sequences were de novo assembled using SPAdes.v.3.12.0 (Nurk et al., 2017) with k-mer values of 21, 33, 55 and 77. The completeness, contamination, and strain heterogeneity of metagenome-assembled genomes (MAGs) were evaluated by using CheckM (version 1.0.5) (Parks et al., 2015). Taxonomy annotation of MAGs obtained from binning was conducted based on the GTDB-Tk database (Chaumeil et al., 2020). Detailed information about the metagenome-assembled genomes is shown in Table S2. For each predicted coding sequence, protein function was annotated using the KEGG server (Kanehisa et al., 2004).

2.9. Statistical analysis

Principal coordinates analysis (PCoA) was used for the analysis of microbial taxonomic compositions, autotrophic microbial composition and *cbbL* OTU distribution. Analysis of variance using distance matrices (Adonis) was used to portion the distance of the soil autotrophic communities and genes among the land-use types. Canonical correspondence analysis (CCA) was used to analyze the effects of soil properties on the distribution of soil microbes. A random forest model was used to analysis the importance of autotrophic populations affiliated with each carbon fixation pathway for the variations of autotrophic microbial

community. Hierarchical cluster analysis based on the Bray-Curtis distance was used to analyze the cluster of soil microbial taxonomic compositions. The random forest model was used to analysis the relative importance of soil properties to ACF rates. The partial least-squares path model (PLSPM) was used to reflect direct or indirect effects of soil properties and microbial community on ACF rates. The resolution of CCA in the R package "rdacca.hp" was used to determine the relative importance of soil properties to ACF rates and autotrophic microbial communities (Lai et al., 2022). Network analysis was performed to investigate the co-occurrence patterns of bacterial and archaeal taxa (Barberán et al., 2012). In the network, a connection indicated a strong ($0.6 < |r| < 1$) and significant ($p < 0.05$) Spearman's correlation between soil microbial families. All statistical analyses were performed using R version 4.0.4 (https://www.r-project.org/) and R packages including "stats", "vegan", "ggrepel", and "igraph". The bar and line plot were graphed using Origin 8.0 (OriginLab, USA).

3. Results

3.1. Microbial $^{13}CO_2$ fixation rate

The δ^{13}C-SOC values of the control soils ranged from –19.29‰ (crop land) to –23.61‰ (grass land), and $^{13}CO_2$ labelling elevated δ^{13}C values of SOC and DOC (Fig. 1). Especially, after incubated for 21 days under light conditions, the δ^{13}C-SOC and δ^{13}C-DOC values in grass land soil increased to 120.9‰ and 1520.7‰, respectively. After 21 days of incubation, the ACF rates in continuous darkness ranged from 0.14 to 0.46 mg C·kg^{-1}·day^{-1}, and ranged from 0.18 to 1.54 mg C·kg^{-1}·day^{-1} in alternate 12 h light with darkness, while largely increased in continuous light conditions (0.24 to 2.57 mg C·kg^{-1}·day^{-1}) (Fig. 2A). Thereinto, the ACF rates were always lowest in bare land and highest in grass land under conditions with and without light. In addition, there was no substantial difference in ACF rates between 7 days and 21 days incubation for each land-use type, except that in grass land under continuous light conditions. And ^{13}C-DOC content in grass land soil was also highest and it was 6.68 times of that in bare land soil in continuous light conditions (Fig. 2B).

3.2. Tracking the fate of $^{13}CO_2$ in SOM using ^{13}C NMR

The ^{13}C NMR analysis showed that the chemical structures of SOM were different among control soils of the four land-use types (Table S4). For example, the SOM of control grass land soil had lower ratios of both aromatic carbon to aliphatic carbon and hydrophobic carbon to hydrophilic carbon. After $^{13}CO_2$ labelling in alternate 12 h light with darkness for 21 days, the ^{13}C NMR signature strengths of the four land-use types soil were higher than those of the control group, and the increased signals mainly included alkyl carbon, alkoxyl carbon, aromatic carbon and carbonyl carbon (Fig. 3A). Remarkably, the increased signals were different among the four land-use types. In bare land, the relative proportion of aromatic carbon was the highest (54.7%) in the total increase of peak intensity. In contrast, the carbonyl carbon was dominant (45.8%) in the total increase of peak intensity in grass land soil. In addition, compared with soils which were $^{13}CO_2$ labelled in continuous darkness, the ^{13}C NMR signals of SOM were apparently higher in soils labelled in continuous light (Fig. 3B). Similarly, the aromatic carbon was dominant in the total increase of peak intensity under light conditions in both bare land and crop land soils, while the increase of alkoxyl carbon was the largest in grass land under light conditions.

3.3. Taxonomic composition of soil microbial community

Taxonomic analysis of the classified ORFs showed that bacteria were dominant in the prokaryotic communities, for example, the main soil microbes at the phylum level were Actinobacteria (49.06%–65.72%), Proteobacteria (8.81%%–17.90%), Gemmatimonadetes (5.25%–10.82%), Chloroflexi (1.74%–3.45%), and Acidobacteria (1.44%–3.05%) (Fig. S2A). While the main archaeal phyla were Thaumarchaeota (0.06%–11.83%) and Euryarchaeota (0.25%–0.37%), and Thaumarchaeota was largely enriched in grass land soil. In addition, the taxonomic compositions of the four land-use types were clearly different (Fig. S2B, $R^2 = 0.90$, $p = 0.001$). The microbial community in grass land soil was positively correlated with most soil properties, including SOC, DOC and TN (Fig. S2C).

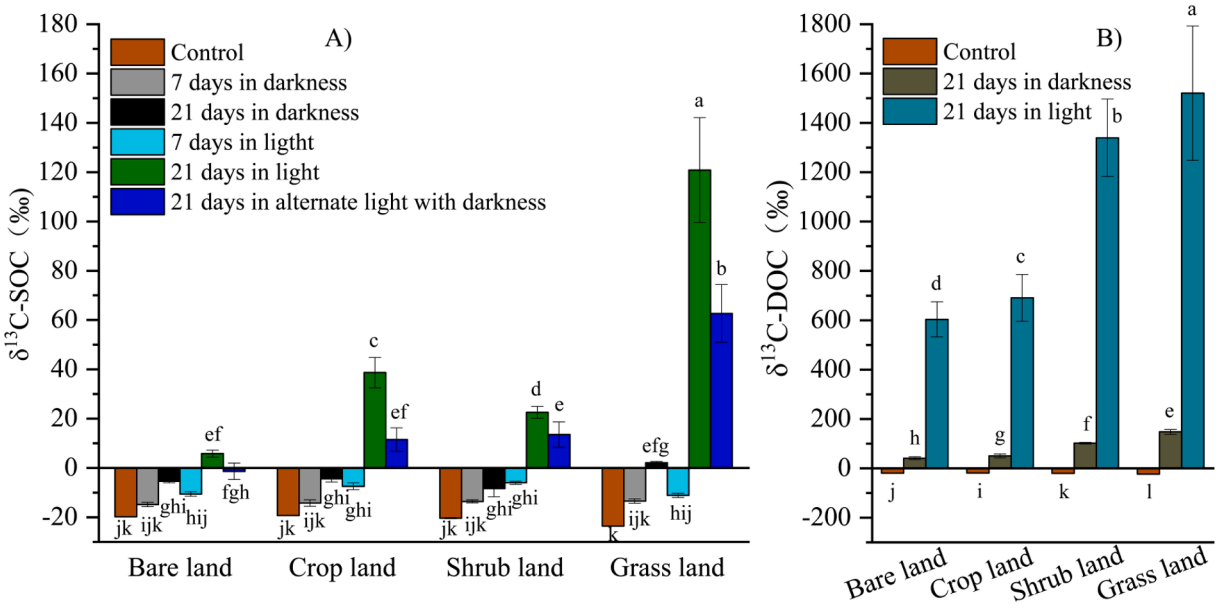

Fig. 1. The δ^{13}C values of SOC (δ^{13}C-SOC, A) and DOC (δ^{13}C-DOC, B) in control and treatments of $^{13}CO_2$ labelling. Data are means ± SD (n = 3).The samples were cultivated for 7 and 21 days at 25 °C. SOC, soil organic carbon; DOC, soil dissolved organic carbon. The differences among the four land-use types were tested by one-way ANOVA, indicated by different letters on the top of column (Duncan; $p < 0.05$).

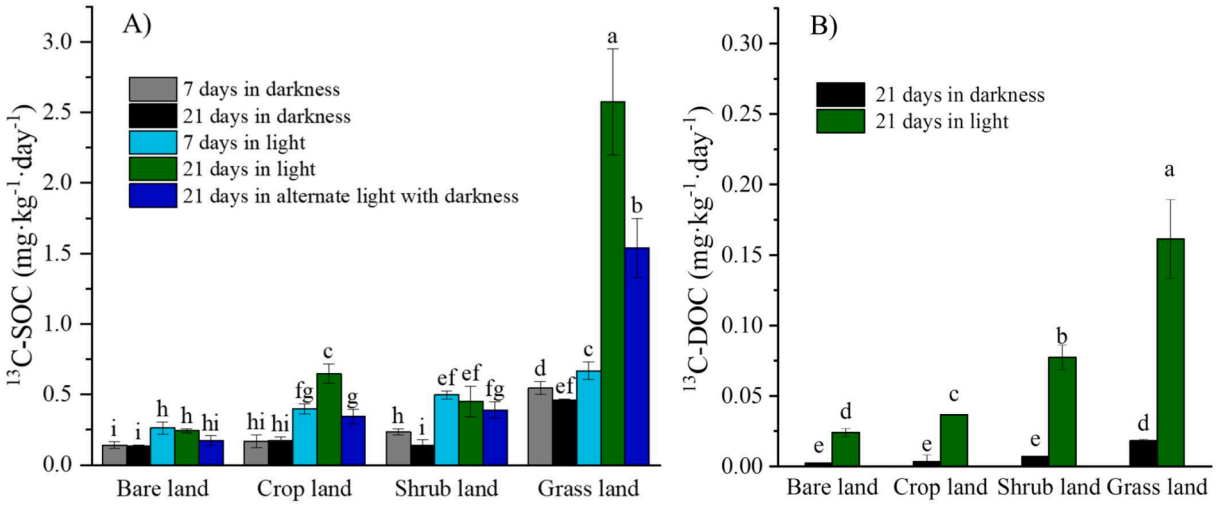

Fig. 2. The rate of $^{13}CO_2$ incorporated into SOC (^{13}C-SOC, mg C·kg^{-1}·day^{-1}) (A) and DOC (^{13}C-DOC, mg C·kg^{-1}·day^{-1}) (B). Data are means ± SD (n = 3). The differences among the four land-use types were tested by one-way ANOVA, indicated by different letters on the top of column (Duncan; $p < 0.05$).

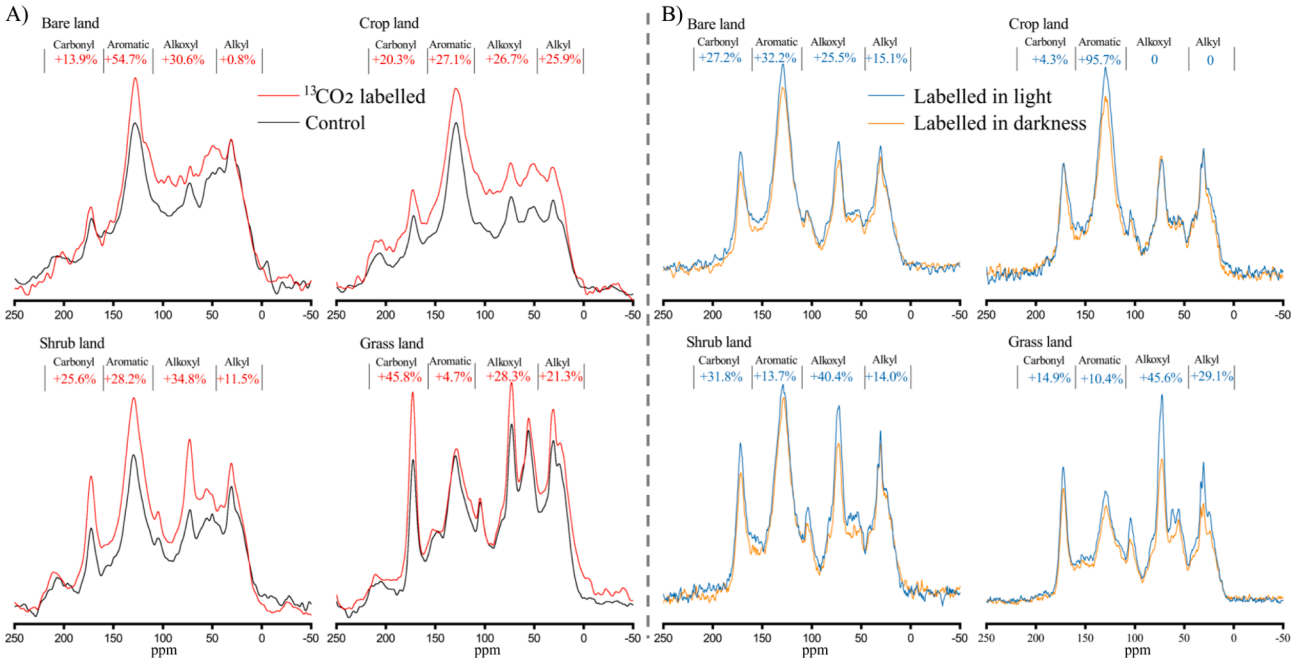

Fig. 3. ^{13}C nuclear magnetic resonance (^{13}C NMR) comparison between $^{12}CO_2$ (control) and $^{13}CO_2$ labelled soils incubated in alternate 12 h light with darkness (A), and between $^{13}CO_2$ labelled soils cultivated under continuous darkness and light conditions (B). The soil samples were cultivated for 21 days. The percentage values of the functional groups represented relative proportion of the increased peak intensity in the total increase of peak intensity after $^{13}CO_2$ labelling, or compared with that labelled in continuous darkness conditions. The NMR spectra were divided into alkyl carbon (0–45 ppm), alkoxyl carbon (45–110 ppm), aromatic carbon (110–160 ppm), and carbonyl carbon (160–210 ppm).

3.4. Putative autotrophic communities and genes

The PCoA analysis indicated that the overall autotrophic communities were prominently different ($R^2 = 0.90$, $p = 0.001$) in the four land-use types (Fig. 4A, Table S5), and the random forest analysis showed that autotrophs affiliated with 3-HP cycle, DC/4-HB cycle and 3-HP/4-HB cycle had the greatest influence on the variations of autotrophic community (Fig. 4B). In addition, the PCoA analysis also showed that the *cbbL*-carrying autotrophic communities were different ($R^2 = 0.52$, $p = 0.001$) among the land-use types (Fig. 4C). The top 5 putative autotrophic microbial families (based on the averaged relative abundances) all belonged to phylum Actinobacteria, including Solirubrobacteraceae (9.56%–13.57%), Nocardioidaceae (7.88%–14.66%), Gemmatimonadaceae (4.58%–10.02%), Conexibacteraceae (4.65%–8.07%) and Rubrobacteraceae (1.72%–9.85%) (Fig. 5 and Table S5). In addition, the putative autotrophic families of Comamonadaceae, Nitrososphaeraceae, Streptomycetaceae, Intrasporangiaceae and Micrococcaceae were apparently enriched in grass land (Fig. 5 and Table S5).

The total relative abundance of genes belonging to the six known carbon fixation pathways was 2.34%–2.80% of the assembled metagenomes, and it was lowest in bare land and highest in grass land soil (Table 2). The relative abundance of rTCA cycle was 0.74%–0.93%, it was about three times of the abundances of CBB cycle and 3-HP/4-HB cycle. The relative abundance of WL pathway was lowest (about 0.08%) in all the land-use types. The analysis of typical microbial families affiliated with each autotrophic carbon fixation pathway indicated

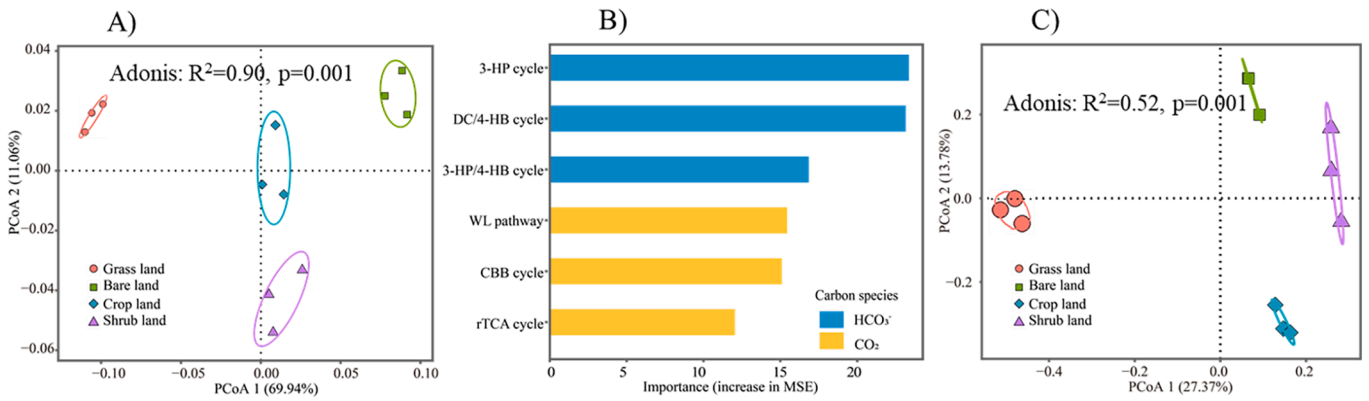

Fig. 4. PCoA of putative autotrophic microbial families related to the six carbon fixation pathways (A), importance (increase in MSE) of autotrophic populations affiliated with each carbon fixation pathway for the variations of autotrophic microbial communities among the four land-use types (B), and PCoA of *cbbL* OTUs based on the unweighted UniFrac distance metric (C). The comparison of difference in microbial communities among the four land-use types using Adonis was shown in the figure. CBB cycle, reductive pentose phosphate cycle; rTCA cycle, reductive citrate cycle; DC/4-HB cycle, dicarboxylate-hydroxybutyrate cycle; 3-HP/4-HB cycle, hydroxypropionate-hydroxybutylate cycle; 3-HP cycle, 3-Hydroxypropionate bi-cycle; WL pathway, reductive acetyl-CoA pathway.

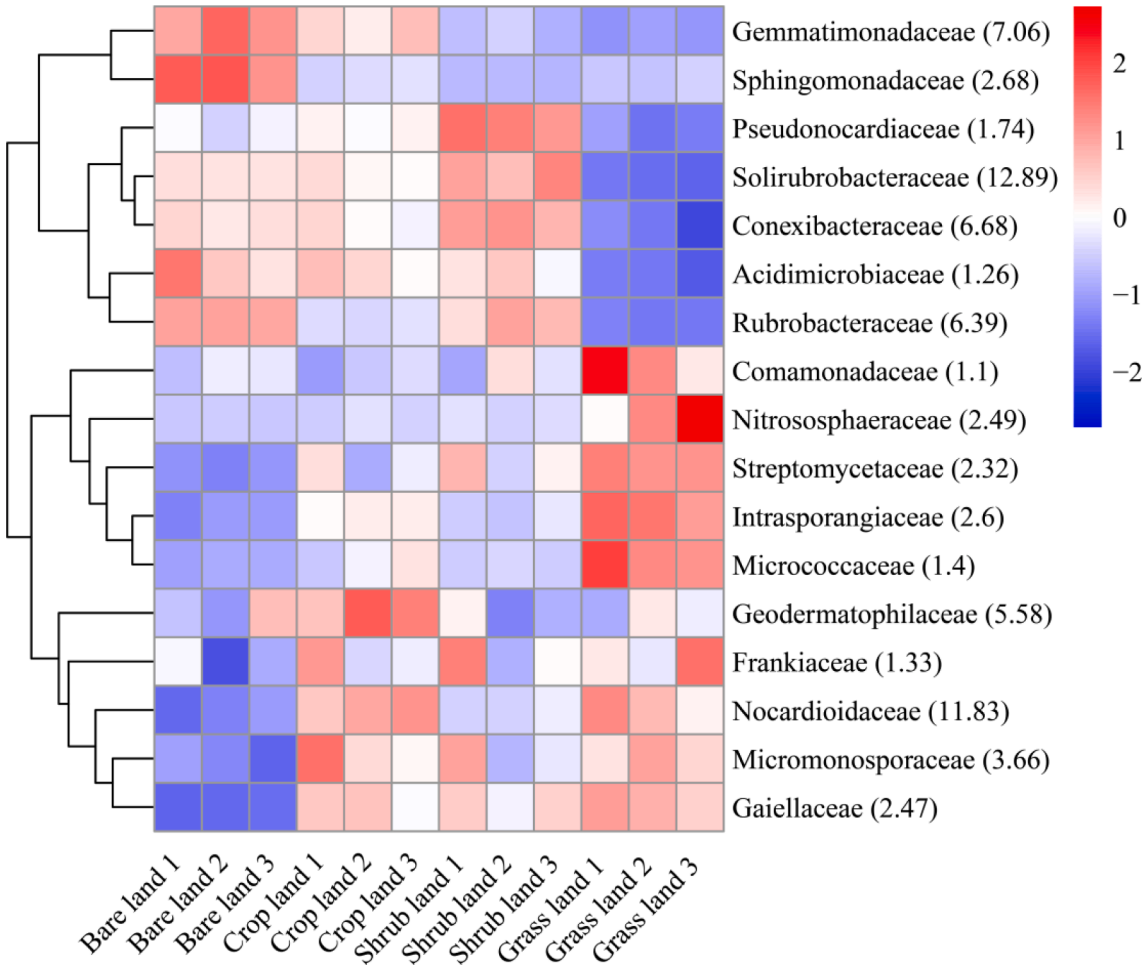

Fig. 5. Heatmap of putative autotrophic families related to the six carbon fixation pathways in the four land-use types. The microbial family displayed in this figure has relative abundance of more than 1% of total autotrophic microbes.

that the microbial families related to the CBB cycle had the lowest abundance in grass land (Fig. 6). In contrast, the Nitrosophaeraceae, which harbored marker genes of both ammoxidation and 3-HP/4-HB cycle, were substantially enriched in grass land soil (Fig. 6 and Fig. S4).

3.5. Correlation among soil land-use type, ACF rate, autotrophic community and genes

The PLSPM analysis showed that soil land-use type directly affected the ACF rate, meanwhile, it could also indirectly affect ACF rate by regulating the autotrophic microbial community and carbon fixation

Table 2
Relative abundance (%) of genes involved in carbon fixation pathways.

	CBB cycle	rTCA cycle	DC/4-HB cycle	3-HP/4-HB cycle	3-HP cycle	WL pathway	Total
Bare land	0.239±0.006b	0.736±0.010c	0.539±0.009 d	0.270±0.004c	0.480±0.010c	0.081±0.001 ab	2.344±0.038 d
Crop land	0.245±0.002 ab	0.815±0.010b	0.587±0.010c	0.302±0.009b	0.524±0.005b	0.079±0.002b	2.552±0.034c
Shrub land	0.249±0.008 a	0.832±0.004b	0.609±0.005b	0.321±0.007 a	0.541±0.005 ab	0.087±0.005 a	2.64±0.017b
Grass land	0.247±0.002 ab	0.931±0.012 a	0.657±0.008 a	0.327±0.013 a	0.553±0.019 a	0.083±0.003 ab	2.798±0.044 a

Data represent the means ± SD (n = 3). CBB cycle, reductive pentose phosphate cycle; rTCA cycle, reductive citrate cycle; DC/4-HB cycle, dicarboxylate-hydroxybutyrate cycle; 3-HP/4-HB cycle, hydroxypropionate-hydroxybutylate cycle; 3-HP cycle, 3-Hydroxypropionate bi-cycle; WL pathway, reductive acetyl-CoA pathway. The differences in relative abundances among the four land-use types were tested by one-way ANOVA, and different letters indicate significant difference (Duncan; $p < 0.05$) between the data.

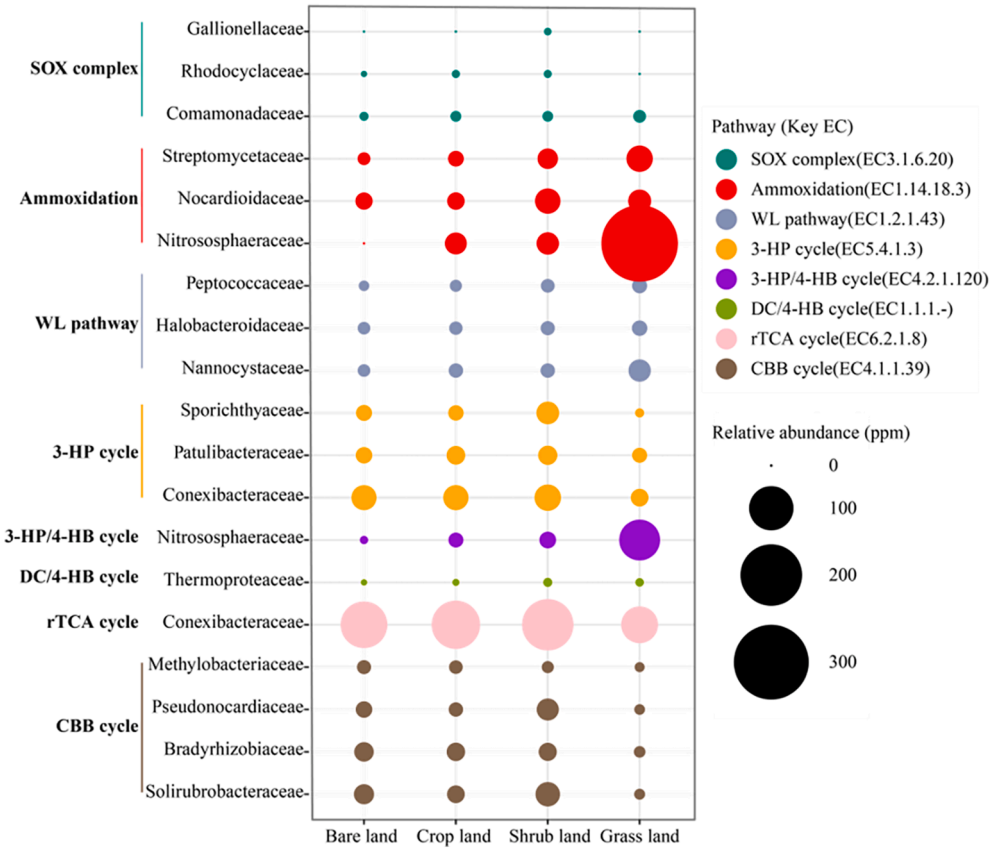

Fig. 6. Relative abundance of typical microbial families affiliated with each autotrophic carbon fixation pathway. The KOs of the marker genes were converted to the Enzyme Commission (EC) numbers. Ammoxidation included nitrification and comammox and its key EC was amoABC. The SOX complex was abbreviation of "thiosulfate oxidation by SOX complex". The sizes of the colored circles are proportional to the relative abundances of the sequences per metagenome, which were computed as proportions of the number of reads to the total number of reads per data set and normalized according to the corresponding gene size.

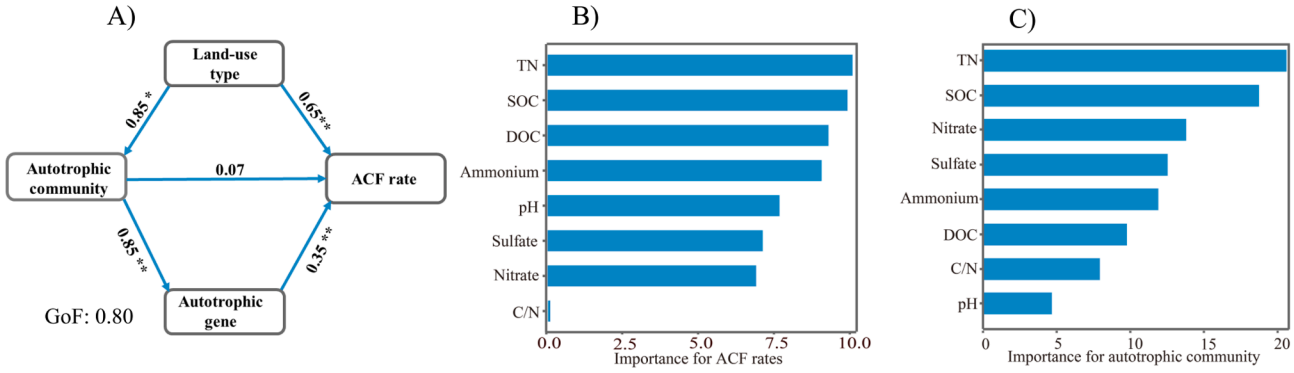

Fig. 7. The partial least-squares path model (PLSPM) showing the direct or indirect effects of soil properties and autotrophic communities on the variation of ACF rates (A). The goodness-of-fit (GoF) of the model is 0.80. The path coefficient represented the direction and strength of direct effect between two variables, *$p < 0.05$, **$p < 0.01$. The relative importance of soil properties to variation of ACF rates (B) and autotrophic communities (C) based on random forest model and R package "rdacca.hp", respectively. The autotrophic genes and communities of each autotrophic carbon fixation pathway were classified according to the marker genes showing in Fig. 6.

pathway (Fig. 7A). Both the contents of TN and SOC were the most important soil properties influencing the variation of ACF rates and autotrophic communities (Fig. 7B and C). Meanwhile, about twenty soil autotrophic microbial families, including Peptococcaceae, Gaiellaceae and Microbacteriaceae, were important nodes in the network of the top 100 soil microbial families (Fig. S5).

4. Discussion

4.1. The importance of ACF rates under darkness and light conditions in karst soil

After $^{13}CO_2$ labelling, apparent increases were observed in both δ^{13}C-SOC and δ^{13}C-DOC across all incubation conditions, especially after 21 days incubation in light (Fig. 1). These observations indicated that autotrophic microbes assimilated the $^{13}CO_2$ into soil organic carbon pool. Furthermore, considering the much greater rise in δ^{13}C-DOC (41.0‰–1520.7‰) compared to δ^{13}C-SOC (-14.8‰–120.9‰) (Fig. 1A and B), we inferred that the assimilated CO_2 was first incorporated into DOC and then converted into macromolecule SOM complexes. Previous studies have also shown that ^{13}C-DOC was assimilated to SOC components which were more stable and more resistant to further degradation (Liang et al., 2017). Moreover, the rapid turnover of newly incorporated ^{13}C-DOC could be helpful in reducing the decomposition of original SOM (Ge et al., 2012). In continuous dark incubation, the ACF rates of the four land-use types were 0.14–0.55 mg C·kg^{-1}·day^{-1} (Fig. 2A), comparable to the dark CO_2 fixation capacity of temperate forest soil (0.5 mg C·kg^{-1}·day^{-1}) (Akinyede et al., 2020). The ACF rates (0.18–1.54 mg C·kg^{-1}·day^{-1}, Fig. 2A) under alternate 12 h light with darkness were on the same order of magnitude as those of subtropical upland and paddy soils (0.18–1.10 mg C·kg^{-1}·day^{-1}) incubated under similar conditions (Ge et al., 2013). Therefore, microbial autotrophic carbon fixation could also be important for SOM in karst soil.

4.2. Land-use types changed the soil properties which then affected the ACF rates in conditions with and without light

Under the incubation duration of 21 days, the ACF rates varied largely among the different land-use types in conditions with and without light (Fig. 2A). The ACF rates in grass land soil, which were always highest under different lighting conditions, increased from 0.46 mg C·kg^{-1}·day^{-1} in darkness to 1.54 mg C·kg^{-1}·day^{-1} under alternate light with darkness, and reached 2.57 mg C·kg^{-1}·day^{-1} in continuous light conditions (Fig. 2A). In contrast, the ACF rates in crop and shrub land soils under continuous light conditions were only elevated to 0.65 and 0.45 mg C·kg^{-1}·day^{-1} respectively. These results indicated that the grass land had both the strongest chemolithotrophic and photoautotrophic ACF rates, which could be explained by the largely elevated contents of TN, SOC, ammonium, etc. in grass land (Table 1). The grass land had highly improved soil properties probably due to that it's dominated by *Alfalfa* (Wang et al., 2021). Previous studies have reported that the higher SOC in desert soil and higher TN in paddy soil significantly promoted the ACF rate (Zhao et al., 2018; Wei et al., 2022). The results of random forest analysis also indicated that contents of TN and SOC were the key controlling factors of the variations of ACF rates (Fig. 7B).

Moreover, the much higher contents of TN and SOC might stimulate substantial propagation of photoautotrophs in surface soil of grass land during longer incubation in light conditions, and lead to largely increased photoautotrophic carbon fixation rate, since earlier study found that the abundance of photoautotrophs in dryland soil crust was positively correlated with soil properties, including TN and SOC (Janatková et al., 2013). These might explain why in grass land, the ACF rate of 21 days incubation (2.57 mg C·kg^{-1}·day^{-1}) was about 4 times of that under 7 days incubation (0.67 mg C·kg^{-1}·day^{-1}) in continuous light (Fig. 2A).

Resultantly, the relative potential of chemolithotrophic versus phototrophic microbial carbon fixation was much lower in grass land, such as, the percentage of ACF rate in continuous dark to light conditions was 18% in grass land after 21 days incubation, while this ratio was higher (27%–56%) in soils of other land-use types (Table S3). Similarly, the δ^{13}C-SOC of each land-use type also indicated that the ACF rates of phototrophic microbes should be largely higher than that of chemolithotrophic microbes, since after 21 days incubation, the δ^{13}C-SOC of all the four land-use types increased to positive values under light conditions, and even reached 120.9 ‰ in grass land, while most of the δ^{13}C-SOC were still negative under dark conditions (Fig. 1A). Meanwhile, the carbon fixed by autotrophic microbes in topsoil should also be important for SOM since it can migrate to deep soil (Davies et al., 2013; Wu et al., 2014). Therefore, our results suggested that by changing the soil properties, the several years of continued land-use practices largely affected both the chemolithotrophic and photoautotrophic microbial carbon fixation.

4.3. $^{13}CO_2$ was incorporated into different components of SOM depending on the land-use types

The fixed CO_2 was mainly incorporated into aliphatic carbon, including carbonyl and alkoxyl carbon of SOM in grass land soil, but it was largely converted into aromatic carbon in soils of other land-use types, especially in bare land soil (Fig. 3A). These results indicated that the SOM components derived from ACF could be easily degradable in grass land soil, but they should be much more stable in other land-use types, since the aliphatic carbon, was considered labile carbon while aromatic carbon was generally a recalcitrant component of SOM (Yao et al., 2019; Yeasmin et al., 2020). Therefore, different land-use types could also affect the fate and stability of the incorporated inorganic carbon in soil by changing the soil properties.

Similarly, the SOM of control grass land soil also contained a higher proportion of alkoxyl carbon, while the control soils of other land-use types had higher proportion of aromatic carbon than grass land (Table S4). The distinct SOM quality among land-use types was previously reported to be explained by their different plant litter and root exudates (Mendham et al., 2002; Yeasmin et al., 2020). However, our results suggested that the CO_2 incorporated by autotrophic microbes might also have important influence on the SOM quality. Besides, the ^{13}C NMR signatures of soils labelled in continuous light conditions were generally higher than those in continuous darkness, suggested that photoautotrophic microbes could make a greater influence on SOM quality (Fig. 3B).

4.4. The land-use types changed the soil properties which then affected the autotrophic community and carbon fixation pathway

Actinobacteria, including Solirubrobacteraceae, Nocardioidaceae, and Conexibacteraceae, were the most important autotrophs (61.6%-74.3% of autotrophs) in soils of the four land-use types (Fig. 5). Recent study also indicated that Actinobacteria could be the most abundant autotrophs in global soils (Bay et al., 2021). Meanwhile, these autotrophic microbes may play an important role in the soil microbial co-occurrence network (Fig. S5). The relative abundance of rTCA cycle was highest (0.736%–0.931%), while WL pathway was lowest (0.079%–0.087%) in soils of these land-use types (Fig. 6). This was consistent with reports on autotrophic carbon fixation pathway in desert and other soils (Liu et al., 2018; Sun et al., 2020). This might be explained by that the rTCA cycle only need 2 ATP to form one molecular pyruvate and prefer microanaerobic environment, but WL pathway was generally limited to strictly anaerobic environment (Berg et al., 2011; Hügler and Sievert, 2011).

However, the autotrophic populations affiliated with carbon fixation pathways of 3-HP cycle, DC/4-HB cycle and 3-HP/4-HB cycle were most important in explaining the variations of the autotrophic microbial

communities among the four land-use types (Fig. 4). Interestingly, all these three carbon fixation pathways use bicarbonate as inorganic carbon species (Berg, 2011; Liu et al., 2018). In fact, inorganic carbon usually exists preferentially in the form of bicarbonate under neutrophilic and alkaliphilic conditions, e.g. in karst soil. Moreover, the substantially higher SOC contents, such as in grass land soil, would lead to much stronger soil respiration (Tian et al., 2022) and higher content of bicarbonate than that in other land-use types (Zeng et al., 2017). Therefore, the content of bicarbonate which would increase with the SOC content might be the key controlling factor for variations of the autotrophic communities among the land-use types in karst soil. So far, there are hardly other studies suggested that the inorganic carbon affected the variations of autotrophic microbial community, although several studies have reported that carbon fixation rate increased with CO_2 concentration (Akinyede et al., 2020; Spohn et al., 2020).

Meanwhile, the substantially higher TN in grass land apparently stimulated the abundance of ammonium oxidizing microbes, including Nitrososphaeraceae, which belongs to Thaumarchaeota and carries out autotrophic metabolism by pathway of 3-HP/4-HB cycle (Fig. 4) (Ruiz-Fernandez et al., 2020). Eventually, the change in contents of TN and SOC might largely explain the influence of land-use types on the soil autotrophic microbial communities and carbon fixation pathways (Fig. 7C).

5. Conclusions

Our results suggested that land-use types changed the soil properties which then largely affected the activity and community of soil autotrophic microbes. Moreover, the change of soil properties caused by land-use type could also determine the fate and stability of the CO_2 assimilated by soil autotrophic microbes. Besides, the TN and SOC contents could be the key factors controlling microbial autotrophic carbon fixation activity and community among different land-use types. Moreover, autotrophic populations assimilating bicarbonate were most influential for the variations of autotrophic communities among the land-use types in karst soils. At last, our study also suggested that longer incubation in light conditions could be important for accurately evaluating the microbial phototrophic CO_2 fixation rates. Further studies with ambient CO_2 concentration and in situ isotopic labelling would facilitate deeper understanding of the activity of autotrophic microbes in karst soils.

Declaration of Competing Interest

The authors declare that they have no known competing financial interests or personal relationships that could have appeared to influence the work reported in this paper.

Data availability

Data will be made available on request.

Acknowledgements

We thank Prof. Ralf Conrad for proof reading and helpful discussion. This work was supported by the Strategic Priority Research Program of Chinese Academy of Sciences (No. XDB40020401); by the National Natural Science Foundation of China (No. 41573083 and U1612441); by the Chinese Academy of Sciences “Light of West China” Program; by the Natural Science Foundation of Education Department of Guizhou Province (No. KY [2018] 255); by the Central Government Leading Local Science and Technology Development Program (QianKeZhongYinDi [2021] 4028).

Appendix A. Supplementary data

Supplementary data to this article can be found online at https://doi.org/10.1016/j.geoderma.2023.116635.

References

Akinyede, R., Taubert, M., Schrumpf, M., Trumbore, S., Küsel, K., 2020. Rates of dark CO_2 fixation are driven by microbial biomass in a temperate forest soil. Soil Biology and Biochemistry 150.
Barberán, A., Bates, S.T., Casamayor, E.O., Fierer, N., 2012. Using network analysis to explore co-occurrence patterns in soil microbial communities. The ISME Journal 6 (2), 343–351.
Bay, S.K., Dong, X.Y., Bradley, J.A., Leung, P.M., Grinter, R., Jirapanjawat, T., Arndt, S. K., Cook, P.L.M., LaRowe, D.E., Nauer, P.A., Chiri, E., Greening, C., 2021. Trace gas oxidizers are widespread and active members of soil microbial communities. Nature Microbiology 6, 246–256.
Berg, I.A., 2011. Ecological aspects of the distribution of different autotrophic CO_2 fixation pathways. Applied and Environmental Microbiology. 77 (6), 1925–1936.
Burst, M., Chauchard, S., Dambrine, E., Dupouey, J.-L., Amiaud, B., 2020. Distribution of soil properties along forest-grassland interfaces: Influence of permanent environmental factors or land-use after-effects? Agriculture, Ecosystems & Environment 289.
Chaumeil, P.-A., Mussig, A.J., Hugenholtz, P., Parks, D.H., Hancock, J., 2020. GTDB-Tk: a toolkit to classify genomes with the Genome Taxonomy Database. Bioinformatics 36 (6), 1925–1927.
Chen, H., Wang, F., Kong, W., Jia, H., Zhou, T., Xu, R.i., Wu, G., Wang, J., Wu, J., 2021. Soil microbial CO_2 fixation plays a significant role in terrestrial carbon sink in a dryland ecosystem: A four-year small-scale field-plot observation on the Tibetan Plateau. The Science of the Total Environment 761.
Davies, L.O., Schäfer, H., Marshall, S., Bramke, I., Oliver, R.G., Bending, G.D., Bertilsson, S., 2013. Light structures phototroph, bacterial and fungal communities at the soil surface. PLoS One 8 (7), e69048.
Degnan, P.H., Ochman, H., 2012. Illumina-based analysis of microbial community diversity. The ISME Journal 6 (1), 183–194.
Edgar, R.C., 2010. Search and clustering orders of magnitude faster than BLAST. Bioinformatics 26 (19), 2460–2461.
Figueroa, I.A., Barnum, T.P., Somasekhar, P.Y., Carlstrom, C.I., Engelbrektson, A.L., Coates, J.D., 2018. Metagenomics-guided analysis of microbial chemolithoautotrophic phosphite oxidation yields evidence of a seventh natural CO_2 fixation pathway. Proceedings of the National Academy of Sciences of the United States of America. 115, 92–101.
Ge, T., Yuan, H., Zhu, H., Wu, X., Nie, S., Liu, C., Tong, C., Wu, J., Brookes, P., 2012. Biological carbon assimilation and dynamics in a flooded rice-Soil system. Soil Biology and Biochemistry 48, 39–46.
Ge, T., Wu, X., Chen, X., Yuan, H., Zou, Z., Li, B., Zhou, P., Liu, S., Tong, C., Brookes, P., Wu, J., 2013. Microbial phototrophic fixation of atmospheric CO_2 in China subtropical upland and paddy soils. Geochimica et Cosmochimica Acta 113, 70–78.
Hart, K.M., Kulakova, A.N., Allen, C.C.R., Simpson, A.J., Oppenheimer, S.F., Masoom, H., Courtier-Murias, D., Soong, R., Kulakov, L.A., Flanagan, P.V., Murphy, B.T., Kelleher, B.P., 2013. Tracking the fate of microbially sequestered carbon dioxide in soil organic matter. Environmental Science & Technology 47 (10), 5128–5137.
Hügler, M., Sievert, S.M., 2011. Beyond the Calvin Cycle: Autotrophic Carbon Fixation in the Ocean. Annual Review Marine Science 3 (1), 261–289.
Huson, D.H., Mitra, S., Ruscheweyh, H.-J., Weber, N., Schuster, S.C., 2011. Integrative analysis of environmental sequences using MEGAN4. Genome Research 21 (9), 1552–1560.
Janatková, K., Řeháková, K., Doležal, J., Šimek, M., Chlumská, Z., Dvorský, M., Kopecký, M., 2013. Community structure of soil phototrophs along environmental gradients in arid Himalaya. Environmental Microbiology 15 (9), 2505–2516.
Kanehisa, M., Goto, S., 2000. KEGG: Kyoto Encyclopedia of Genes Genomes. Nucleic Acids Research 28, 27–30.
Kanehisa, M., Goto, S., Kawashima, S., Okuno, Y., Hattori, M., 2004. The KEGG resource for deciphering the genome. Nucleic Acids Research 32, 277–280.
Karlsson, F.H., Tremaroli, V., Nookaew, I., Bergström, G., Behre, C.J., Fagerberg, B., Nielsen, J., Bäckhed, F., 2013. Gut metagenome in European women with normal, impaired and diabetic glucose control. Nature 498 (7452), 99–103.
Kelleher, B.P., Flanagan, P.V., Hart, K.M., Simpson, A.J., Oppenheimer, S.F., Murphy, B. T., O'Reilly, S.S., Jordan, S.F., Grey, A., Ibrahim, A., Allen, C.C.R., 2017. Large perturbations in CO_2 flux and subsequent chemosynthesis are induced in agricultural soil by the addition of elemental sulfur. Scientific Reports 7, 4732.
Lai, J., Zou, Y., Zhang, J., Peres-Neto, P.R., 2022. Generalizing hierarchical and variation partitioning in multiple regression and canonical analyses using the rdacca.hp R package. Methods in Ecology and Evolution 13, 782–788.
Langmead, B., Salzberg, S.L., 2012. Fast gapped-read alignment with Bowtie 2. Nature Methods 9 (4), 357–359.
Li, S.-L., Liu, C.-Q., Chen, J.-A., Wang, S.-J., 2021. Karst ecosystem and environment: Characteristics, evolution processes, and sustainable development. Agriculture, Ecosystems & Environment 306, 107173.
Liang, C., Schimel, J.P., Jastrow, J.D., 2017. The importance of anabolism in microbial control over soil carbon storage. Nature Microbiology 2, 17105.
Liu, Z., Sun, Y., Zhang, Y., Feng, W., Lai, Z., Fa, K., Qin, S., 2018. Metagenomic and ^{13}C tracing evidence for autotrophic atmospheric carbon absorption in a semiarid desert. Soil Biology and Biochemistry 125, 156–166.

Long, X.-E., Yao, H., Wang, J., Huang, Y., Singh, B.K., Zhu, Y.-G., 2015. Community structure and soil pH determine chemoautotrophic carbon dioxide fixation in drained paddy soils. Environmental Science & Technology 49 (12), 7152–7160.
Mendham, D.S., Mathers, N.J., O'Connell, A.M., Grove, T.S., Saffigna, P.G., 2002. Impact of land-use on soil organic matter quality in south-western Australia-characterization with ^{13}C CP/MAS NMR spectroscopy. Soil Biology and Biochemistry 34 (11), 1669–1673.
Miltner, A., Kopinke, F.-D., Kindler, R., Selesi, D., Hartmann, A., Kästner, M., 2005. Non-phototrophic CO_2 fixation by soil microorganisms. Plant and Soil 269 (1-2), 193–203.
Nowak, M.E., Beulig, F., von Fischer, J., Muhr, J., Küsel, K., Trumbore, S.E., 2015. Autotrophic fixation of geogenic CO_2 by microorganisms contributes to soil organic matter formation and alters isotope signatures in a wetland mofette. Biogeosciences 12, 7169–7183.
Nurk, S., Meleshko, D., Korobeynikov, A., Pevzner, P.A., 2017. metaSPAdes: a new versatile metagenomic assembler. Genome Research 27 (5), 824–834.
Ortiz, M., Legatzki, A., Neilson, J.W., Fryslie, B., Nelson, W.M., Wing, R.A., Soderlund, C. A., Pryor, B.M., Maier, R.M., 2014. Making a living while starving in the dark: metagenomic insights into the energy dynamics of a carbonate cave. The ISME Journal 8 (2), 478–491.
Parks, D.H., Imelfort, M., Skennerton, C.T., Hugenholtz, P., Tyson, G.W., 2015. CheckM: assessing the quality of microbial genomes recovered from isolates, single cells, and metagenomes. Genome Research 25 (7), 1043–1055.
Peng, Y.u., Leung, H.C.M., Yiu, S.M., Chin, F.Y.L., 2012. IDBA-UD: a de novo assembler for single-cell and metagenomic sequencing data with highly uneven depth. Bioinformatics 28 (11), 1420–1428.
Peng, T., Wang, S.-J., 2012. Effects of land use, land cover and rainfall regimes on the surface runoff and soil loss on karst slopes in southwest China. Catena 90, 53–62.
Prietzel, J., Muller, S., Kogel-Knabner, I., Thieme, J., Jaye, C., Fischer, D., 2018. Comparison of soil organic carbon speciation using C NEXAFS and CPMAS ^{13}C NMR spectroscopy. The Science of the Total Environment 628–629, 906–918.
Ruiz-Fernandez, P., Ramirez-Flandes, S., Rodriguez-Leon, E., Ulloa, O., 2020. Autotrophic carbon fixation pathways along the redox gradient in oxygen-depleted oceanic waters. Environmental Microbiology Reports. 12, 334–341.
Salati, S., Adani, F., Cosentino, C., Torri, G., 2008. Studying soil organic matter using ^{13}C CP-MAS NMR: the effect of soil chemical pre-treatments on spectra quality and representativity. Chemosphere 70 (11), 2092–2098.
Spohn, M., Müller, K., Höschen, C., Mueller, C.W., Marhan, S., 2020. Dark microbial CO_2 fixation in temperate forest soils increases with CO_2 concentration. Global Change Biology 26 (3), 1926–1935.
Sun, X., Kong, T., Häggblom, M.M., Kolton, M., Li, F., Dong, Y., Huang, Y., Li, B., Sun, W., 2020. Chemolithoautotropic diazotrophy dominates the nitrogen fixation process in mine tailings. Environmental Science & Technology 54 (10), 6082–6093.
Tian, P., Zhao, X., Liu, S., Sun, Z., Jing, Y., Wang, Q., 2022. Soil microbial respiration in forest ecosystems along a north-south transect of eastern China: Evidence from laboratory experiments. Catena 211.
Wang, L., Xie, J., Luo, Z., Niu, Y., Coulter, J.A., Zhang, R., Lingling, L.i., 2021. Forage yield, water use efficiency, and soil fertility response to alfalfa growing age in the semiarid Loess Plateau of China. Agricultural Water Management 243.
Wei, L., Ge, T., Zhu, Z., Ye, R., Peñuelas, J., Li, Y., Lynn, T.M., Jones, D.L., Wu, J., Kuzyakov, Y., 2022. Paddy soils have a much higher microbial biomass content than upland soils: A review of the origin, mechanisms, and drivers. Agriculture, Ecosystems & Environment 326.
Wu, X., Ge, T., Wang, W., Yuan, H., Wegner, C.E., Zhu, Z., Whiteley, A.S., Wu, J., 2015. Cropping systems modulate the rate and magnitude of soil microbial autotrophic CO_2 fixation in soil. Frontiers in Microbiology 6, 00379.
Xiao, K.Q., Ge, T.D., Wu, X.H., Peacock, C.L., Zhu, Z.K., Peng, J., Bao, P., Wu, J.S., Zhu, Y. G., 2020. Metagenomic and ^{14}C tracing evidence for autotrophic microbial CO_2 fixation in paddy soils. Environmental Microbiology 21, 15204.
Yao, S.H., Zhang, Y.L., Han, Y., Han, X.Z., Mao, J.D., Zhang, B., 2019. Labile and recalcitrant components of organic matter of a Mollisol changed with land use and plant litter management: An advanced ^{13}C NMR study. The Science of the Total Environment 660, 1–10.
Yeasmin, S., Singh, B., Smernik, R.J., Johnston, C.T., 2020. Effect of land use on organic matter composition in density fractions of contrasting soils: A comparative study using ^{13}C NMR and DRIFT spectroscopy. The Science of the Total Environment 726.
Yuan, H., Ge, T., Chen, C., O'Donnell, A.G., Wu, J., 2012. Significant role for microbial autotrophy in the sequestration of soil carbon. Applied and Environmental Microbiology 78 (7), 2328–2336.
Zeng, Q., Liu, Z., Chen, B., Hu, Y., Zeng, S., Zeng, C., Yang, R., He, H., Zhu, H., Cai, X., Chen, J., Ou, Y., 2017. Carbonate weathering-related carbon sink fluxes under different land uses: A case study from the Shawan Simulation Test Site, Puding, Southwest China. Chemical Geology 474, 58–71.
Zhao, K., Kong, W.D., Wang, F., Long, X.E., Guo, C.Y., Yue, L.Y., Yao, H.Y., Dong, X.B., 2018. Desert and steppe soils exhibit lower autotrophic microbial abundance but higher atmospheric CO_2 fixation capacity than meadow soils. Soil Biology and Biochemistry 127, 230–238.
Zhao, Y., Liu, P., Rui, J., Cheng, L., Wang, Q., Liu, X., Yuan, Q., 2020. Dark carbon fixation and chemolithotrophic microbial community in surface sediments of the cascade reservoirs, Southwest China. The Science of the Total Environment 698.